

association observed in wild-type cells was missing in the mutant (Fig. 3C, fig. S5). The missing late S phase peak was not due to an absence of telomere-bound Cdc13p, as we observed no difference in telomere binding between *cdc13-2* protein and wild type Cdc13p (17). For Est1p, cell cycle ChIP showed that, if anything, telomere binding was slightly enhanced at most time points in *cdc13-2* cells (Fig. 3C, fig. S5). The *cdc13-2* allele is deficient in interaction with Stn1p (20). It is possible that the increase in Est1p telomere association in *cdc13-2* cells reflects increased telomere accessibility due to a lack of steric hindrance from Stn1p. Regardless, from these data we conclude that Est1p is fully able to associate with telomeres in a *cdc13-2* background.

Telomerase action is not observed in G<sub>1</sub> phase cells, yet we observed strong *TLC1*-dependent telomere association of Est2p, the catalytic subunit, at that time point (Figs. 2 and 3, fig. S2). Access of the Est2p-*TLC1* RNA complex to chromosome ends is, therefore, not sufficient for telomerase action in vivo. The Est2p signal was decreased, but not eliminated, in early S phase, reflecting either dissociation of Est2p from a subset of telomeres or decreased cross-linking efficiency, possibly through a change in conformation or in neighboring components of telomeric chromatin. We observed a second peak of Est2p telomere association in late S phase (Fig. 2B). The fact that this peak did not occur in the telomerase-defective *cdc13-2* background suggests that it reflects an essential process for telomerase action in vivo (Fig. 3C, fig. S5). Our findings suggest that two key events are concurrent with the late S phase Est2p peak: multimerization of Cdc13p on the G tail and Est1p binding. We propose that Est1p is a cell cycle regulated (Fig. 2A) activator of telomerase that binds to an inactive, telomere-bound Est2p-*TLC1* RNA complex in late S phase and then interacts with one or more Cdc13p molecules arrayed on the G tail. This interaction changes the state of bound Est2p, either through binding of additional Est2p (e.g., dimerization) (21) or a conformational change that enhances cross-linking; this is manifested as the late S phase peak of Est2p telomere association and results in activation of telomerase for synthesis. The *cdc13-2* mutation disrupts a functional interaction with Est1p (6). Because Est1p telomere association is robust in *cdc13-2* cells (Fig., 3, B and C), this functional interaction must be separable from and downstream of Est1p telomere binding. We propose the telomerase deficiency of the *cdc13-2* allele reflects failure to interact properly with telomere bound Est1p to promote activation, resulting in persistence of inactive Est2p at the telomere and concurrent loss of the late S phase peak. We detected decreased but still

considerable Est2p telomere association after S phase (Fig. 2B; fig. S2), suggesting that at least a subset of Est2p remains bound to telomeres for the remainder of the cell cycle, perhaps as a protective cap (21). Because the G<sub>1</sub> peak of association followed low association in M phase (17), Est2p appears to load onto telomeres again at the beginning of the next cell cycle.

References and Notes

1. V. A. Zakian, *Science* **270**, 1601 (1995).
2. R. J. Wellinger, K. Ethier, P. Labrecque, V. A. Zakian, *Cell* **85**, 423 (1996).
3. C. I. Nugent, V. Lundblad, *Genes Dev.* **12**, 1073 (1998).
4. S. K. Evans, V. Lundblad, *Science* **286**, 117 (1999).
5. H. Qi, V. A. Zakian, *Genes Dev.* **14**, 1777 (2000).
6. E. Pennock, K. Buckley, V. Lundblad, *Cell* **104**, 387 (2001).
7. S. J. Diede, D. E. Gottschling, *Cell* **99**, 723 (1999).
8. S. Marcand, V. Brevet, C. Mann, E. Gilson, *Curr. Biol.* **10**, 487 (2000).
9. O. M. Aparicio, D. M. Weinstein, S. P. Bell, *Cell* **91**, 59 (1997).
10. M. N. Conrad, J. H. Wright, A. J. Wolf, V. A. Zakian, *Cell* **63**, 739 (1990).
11. J. H. Wright, D. E. Gottschling, V. A. Zakian, *Genes Dev.* **6**, 197 (1992).

12. Y. Tsukamoto, A. K. P. Taggart, V. A. Zakian, *Curr. Biol.* **11**, 1328 (2001).
13. Materials and Methods are available as supporting online material on Science Online.
14. S. Strahl-Bolsinger, A. Hecht, K. Luo, M. Grunstein, *Genes Dev.* **11**, 83 (1997).
15. B. D. Bourms, M. K. Alexander, A. M. Smith, V. A. Zakian, *Mol. Cell. Biol.* **18**, 5600 (1998).
16. T. R. Hughes, R. G. Weilbaecher, M. Walterscheid, V. Lundblad, *Proc. Natl. Acad. Sci. U.S.A.* **97**, 6457 (2000).
17. A. K. P. Taggart, V. A. Zakian, unpublished data.
18. P. T. Spellman *et al.*, *Mol. Biol. Cell* **9**, 3273 (1998).
19. C. I. Nugent, T. R. Hughes, N. F. Lue, V. Lundblad, *Science* **274**, 249 (1996).
20. A. Chandra, T. R. Hughes, C. I. Nugent, V. Lundblad, *Genes Dev.* **15**, 404 (2001).
21. J. Prescott, E. Blackburn, *Genes Dev.* **11**, 2790 (1997).
22. We thank M. K. Alexander, H. Qi, W. H. Tham, S. Schnakenberg, and L. Vega for critical reading of the manuscript. This work was supported by the National Institutes of Health grant GM43265 (to V.A.Z.). A.K.P.T was supported in part by a postdoctoral fellowship from the Susan G. Komen Breast Cancer Foundation and also NIH grant T32 CA09528-16.

Supporting Online Material

www.sciencemag.org/cgi/content/full/297/5583/1023/DC1  
 Materials and Methods  
 Figs. S1 to S5  
 Table S1

11 June 2002; accepted 3 July 2002

## Orc6 Involved in DNA Replication, Chromosome Segregation, and Cytokinesis

Supriya G. Prasanth, Kannanganattu V. Prasanth, Bruce Stillman\*

Origin recognition complex (ORC) proteins serve as a landing pad for the assembly of a multiprotein prereplicative complex, which is required to initiate DNA replication. During mitosis, the smallest subunit of human ORC, Orc6, localizes to kinetochores and to a reticular-like structure around the cell periphery. As chromosomes segregate during anaphase, the reticular structures align along the plane of cell division and some Orc6 localizes to the midbody before cells separate. Silencing of Orc6 expression by small interfering RNA (siRNA) resulted in cells with multipolar spindles, aberrant mitosis, formation of multinucleated cells, and decreased DNA replication. Prolonged periods of Orc6 depletion caused a decrease in cell proliferation and increased cell death. These results implicate Orc6 as an essential gene that coordinates chromosome replication and segregation with cytokinesis.

The initiation of DNA replication in eukaryotic cells is a highly regulated process that leads to the duplication of the genetic information for the next cell generation. Duplication of chromosomes in S phase is followed by segregation of the resultant sister chromatids during mitosis (1). Initiation of DNA replication is mediated by a conserved set of proteins, including ORC, which is bound to origins of DNA replication and is highly conserved (2-4). In human cells, ORC consists of six subunits. In *Drosophila*

embryos, Orc6 forms a complex with other ORC subunits, but there is a major fraction of Orc6 that is not part of the ORC complex, a function for which is hitherto unknown (5, 6). Although ORC acts as a DNA replication initiator protein, it is known to function in other cellular processes such as transcriptional gene silencing and heterochromatin formation (2). To function in DNA replication, ORC proteins need to be recruited to chromatin, but their fate during mitosis has not been clearly established.

We used immunofluorescence to investigate the cell cycle localization of Orc6 protein in human cells. The polyclonal antibody to Orc6 (anti-Orc6) (7) was highly specific (fig. S1). Orc6 was localized in the nucleus

Cold Spring Harbor Laboratory, 1 Bungtown Road, Cold Spring Harbor, NY 11724, USA.

\*To whom correspondence should be addressed. E-mail: stillman@cshl.org

## REPORTS

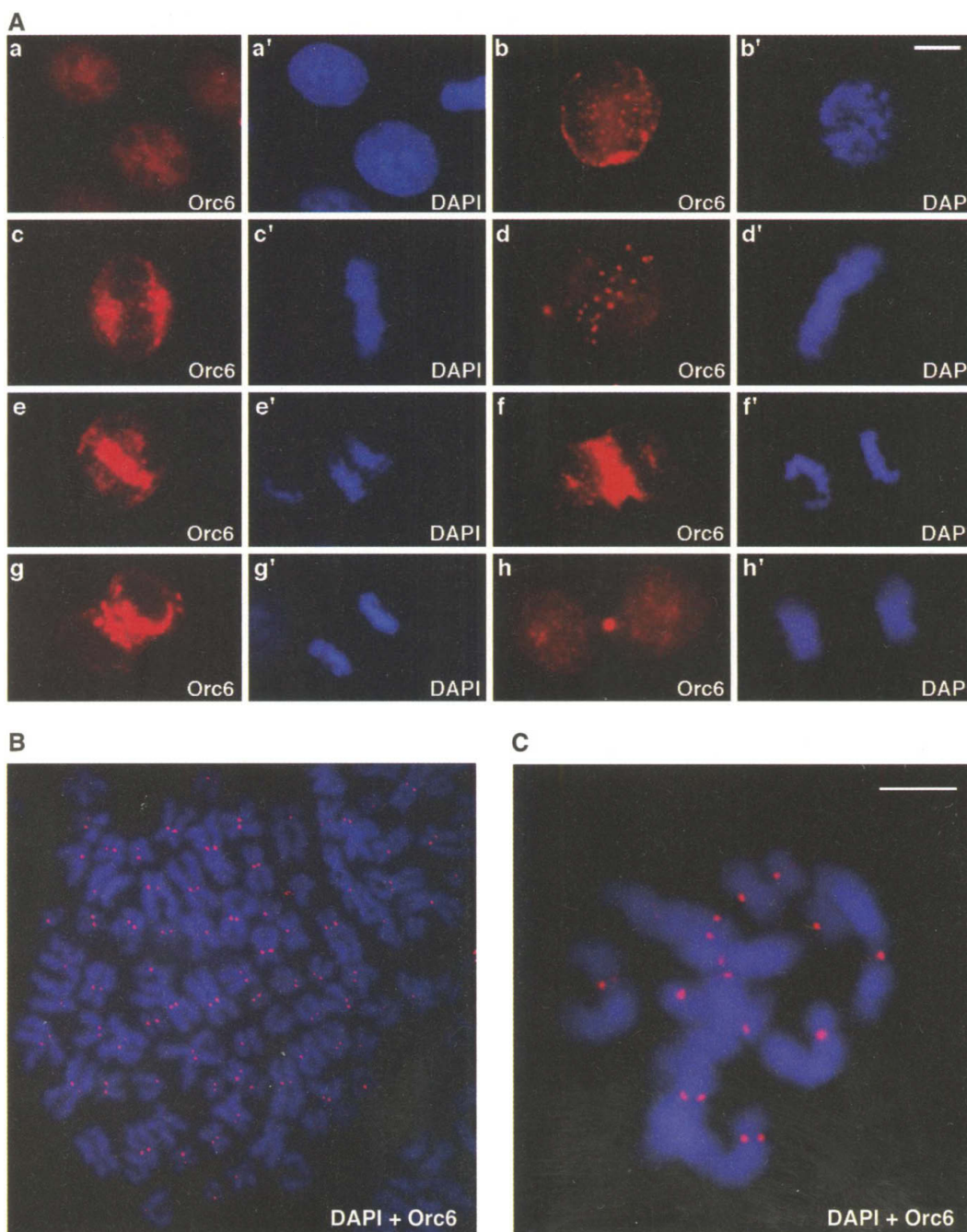
during interphase (Fig. 1A, a). During prophase and during later stages of mitosis, a fraction of the Orc6 protein showed a reticular-like pattern around the cell periphery (Fig. 1A, b). A similar pattern has been reported for *Drosophila* Orc6 (6). The reticular structure containing Orc6 was adjacent to the chromatin during metaphase (Fig. 1A, c) as well as during early and late anaphase in a position that defined the eventual cell division plane at cytokinesis. By late anaphase the Orc6 reticular structures aggregated, became larger, and were mostly present at the midzone (Fig. 1A, e to g). Orc6 began to redistribute to the daughter nuclei by telophase (Fig. 1A, h), but a subset of Orc6

localized to the midzone between the joined cells to form the midbody (Fig. 1A, h). In addition to the reticular-like pattern, from prophase through anaphase, Orc6 showed a punctate pattern on chromosomes (Fig. 1A, b to f) resembling the localization of centromere binding proteins (8). By telophase, Orc6 no longer showed the punctate pattern. Similar observations for Orc6 were made in primary fibroblasts IMR-90 and FHs 738lu and in tumor-derived U2OS and MCF7 cells (9). In addition, the centrosomic localization of Orc6 was confirmed on metaphase spreads of HeLa cells (Fig. 1B) and in a rat kangaroo

cell line, pTK2 (Fig. 1C); these findings suggest evolutionary conservation of the regulated localization of this protein in mammalian cells.

Centromeres are sites of kinetochore assembly, and the centromere-kinetochore complex integrates regulatory signals required for mitotic progression (8). Costaining with antisera to the inner kinetochore from patients with calcinosis, Raynaud's phenomenon, esophageal dysmotility, sclerodactyly, and telangiectasia (collectively abbreviated as CREST) and anti-Orc6 showed significant, but not precise, overlap (Fig. 2, a to c). The paired foci of Orc6 on the aligned sister

**Fig. 1.** Cell cycle distribution of Orc6. **(A)** Cells were fixed with 1.7% paraformaldehyde; immunostaining was carried out according to standard protocols. Indirect immunofluorescence localization (red) of Orc6 proteins is shown in HeLa cells during interphase (a), prophase (b), metaphase [(c and d), where (c) highlights the reticulate pattern of Orc6 distribution and (d) shows the kinetochore pattern during metaphase], early anaphase (e), late anaphase (f), early telophase (g), and telophase (h). The images were observed at different focal planes in round mitotic cells, so patterns may vary between images. In (a') to (h'), chromatin was stained with 4',6'-diamidino-2-phenylindole (DAPI) (blue). Scale bar, 5  $\mu$ m. **(B)** Immunofluorescent localization of Orc6 protein in HeLa metaphase chromosomes shows a doublet characteristic of centromere binding proteins. **(C)** Orc6 immunofluorescence in rat kangaroo pTK2 cell chromosomes, showing centromere binding in metaphase spreads. Orc6 (red) was detected at the primary constriction as two dots per chromosome (DAPI in blue). Scale bar, 5  $\mu$ m.



## REPORTS

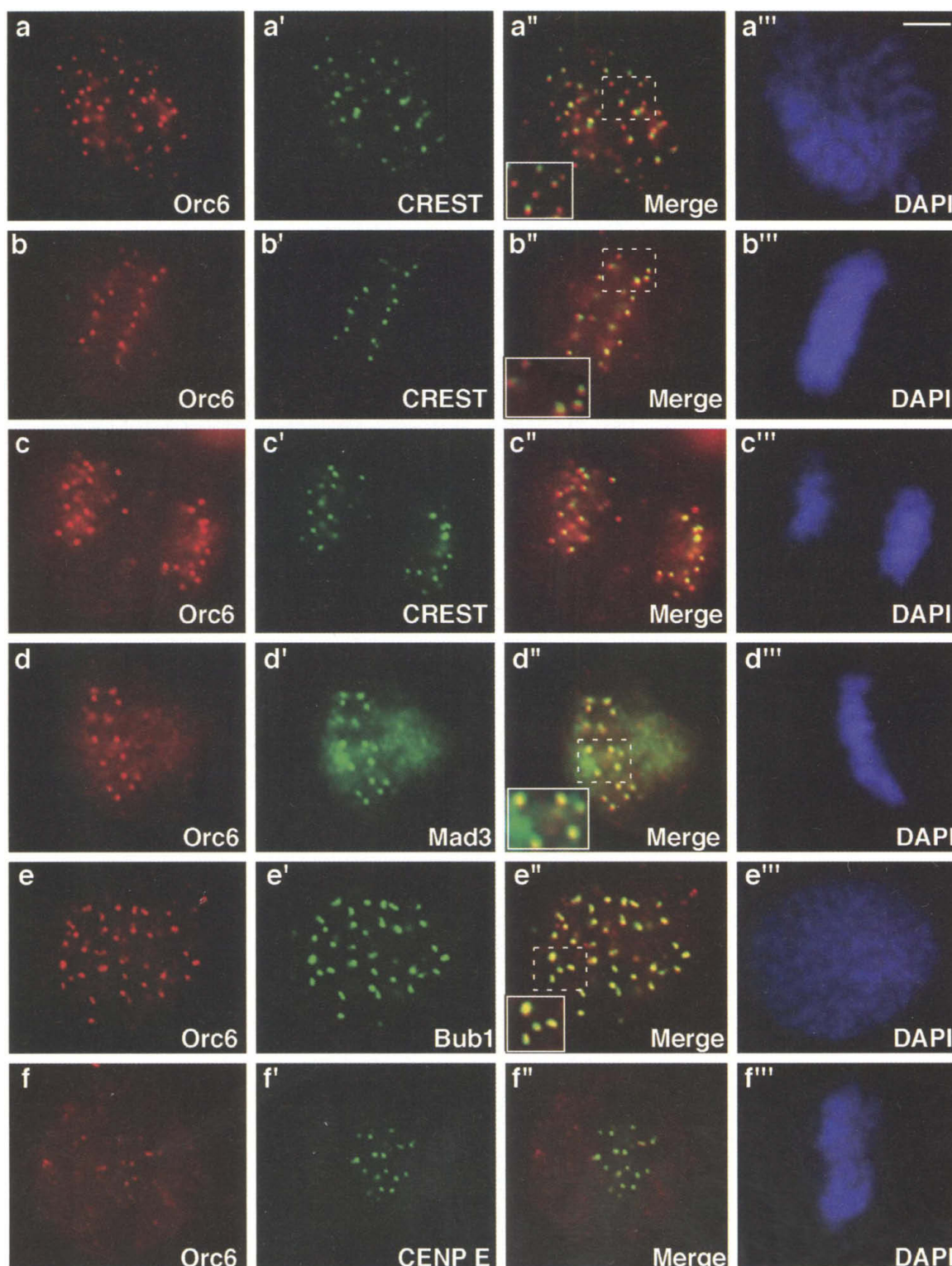
chromatids during metaphase showed that the distance between the spots was greater than the distance to the inner kinetochore CREST doublet (Fig. 2, b''). Double immunostaining of Orc6 and outer kinetochore proteins, including the mitotic checkpoint kinases Mad3 (also referred to as Bub1R) (Fig. 2, d to d''') and Bub1 (Fig. 2, e to e''') and the motor

protein CENP E (Fig. 2, f to f'''), showed significant colocalization, seen as yellow areas (Fig. 2, d'', e'', and f''). The outer kinetochore is a distinct and transitory domain of each centromere that forms at prophase, functions during the ensuing stages of mitosis, and disassembles at the end of mitosis (10). The centromeric localization of Orc6 during

mitosis suggests that it associates with the outer kinetochore. In interphase cells, we did not detect any colocalization of Orc6 foci and centromeres.

Cytokinesis is one of the most striking morphological transformations occurring during cell division (11). The last stage of cytokinesis requires resolving the midbody, a

**Fig. 2.** Kinetochore localization of Orc6 during prophase (a and e), metaphase (b, d, and f), and anaphase (c). Dual-color indirect immunofluorescence analysis used anti-Orc6 (red, a to f) together with CREST (green, a' to c'), Mad3 (d'), Bub1 (e'), or CENP E (f'). Cells were fixed with 0.5% paraformaldehyde for prominent kinetochore staining of Orc6, under which the reticular staining is reduced. For CENP E staining, cells were pre-extracted in 0.2% Triton X-100, followed by fixation and standard antibody staining conditions (27). Under these conditions, Orc6 staining decreased considerably. Merges (a'' to f'') highlight the areas of colocalization (yellow). Insets in a'', b'', d'', and e'' are higher magnification of the boxed portion of the image, showing closer localization of Orc6 to the outer than to the inner kinetochore. Chromatin was stained with DAPI (blue) (a''' to f'''). Scale bar, 5  $\mu$ m.



REPORTS

slender tube of cytoplasm with a phase-dense Flemming body at its center that forms an intercellular bridge between two incipient daughter cells (12). Proteins at the midbody are known to provide molecular cues for the spatial control of cytokinesis and for coordinating the transition from mitosis to the G<sub>1</sub> phase of the cell cycle (12). Immunostaining studies revealed a reticular pattern of Orc6 in the cleavage furrow during anaphase, finally concentrating at the Flemming body in telophase. The localization of Orc6 protein (Fig. 3A) with the known midbody-associated proteins actin (Fig. 3A, a') and ubiquitin (Fig. 3A, b') showed Orc6 at the Flemming body (Fig. 3A, a and b). Survivin, a chromosomal passenger protein that also localizes with kinetochores (13), flanks Orc6 within the Flemming body (Fig. 3A, c'). In contrast, CENP E precisely colocalized with Orc6 at the Flemming body (Fig. 3A, d''). Transiently expressed yellow fluorescent protein (YFP)-Orc6 fusion protein in HeLa cells showed similar patterns of localization (fig. S2). Biochemically purified midbodies from HeLa cells (14) were also positive for Orc6 (Fig. 3B) (fig. S3).

The presence of Orc6 at the kinetochore and its subsequent aggregation at the midzone during the metaphase-anaphase transition suggests that it is functionally related to the class of chromosomal passenger proteins. Members of this class, which include INCENP, survivin, Aurora kinase, and TD-60,

show similar dynamic distribution in mitosis (15). This suggests that Orc6 might coordinate chromosome replication and segregation with cytokinesis.

In *Saccharomyces cerevisiae*, Orc6 is an essential gene, but in vitro it is not required for ORC binding to the origins of DNA replication (16). Yeast Orc6, however, undergoes cell cycle-regulated phosphorylation by cyclin-dependent protein kinase and is dephosphorylated as cells exit mitosis (17). The *Drosophila* Orc6 is required for ORC DNA binding (6) but is not required for replication licensing in *Xenopus* (18). Thus, Orc6 may be involved in function(s) other than initiation of DNA replication.

To assess the importance of the regulated subcellular localization of human Orc6 protein, we transfected Orc6 siRNAs into asynchronously growing HeLa cells (19, 20). Immunoblot analysis of treated cells showed that Orc6 was greatly decreased by 48 hours (after two rounds of transfection) and almost completely lost by 72 hours (after three rounds of transfection; Fig. 4A). In contrast, Orc2 and  $\alpha$ -tubulin proteins did not show any change in cells treated with Orc6 siRNA (Fig. 4A). The cells transfected with G13 siRNA as control showed normal levels of Orc6, Orc2, and  $\alpha$ -tubulin proteins (Fig. 4A, lanes 3, 6, and 9). Immunostaining with anti-Orc6 corroborated the immunoblot results, showing knockdown of Orc6 staining (figs. S4 and S5).

The phenotypes observed after Orc6

siRNA treatment were complex, revealing defects at multiple stages of the mitotic cycle, and varied with time of siRNA treatment. Two sets of Orc6 siRNA duplexes revealed similar phenotypes with insignificant variations. Orc6 siRNA treatment caused increased polyploidy (Fig. 4B; Fig. 4C, a to f) and the number of multinucleate cells increased to 32% by 120 hours after siRNA treatment (Fig. 4B). In addition, silencing of Orc6 expression resulted in cells with multipolar spindles (Fig. 4C, g and h) and aberrant mitosis (Fig. 4C, i). Strikingly, in many Orc6 siRNA-treated cells (at 150 hours), the ability of chromosomes to align in a metaphase plate was abolished (Fig. 4C, j). Prolonged periods of Orc6 depletion caused a decrease in cell proliferation and increased cell death.

Similar studies based on RNA interference (RNAi) carried out with *Drosophila* INCENP and Aurora B showed defects in chromosome alignment, segregation, and cytokinesis (21). In addition, null embryos of mice lacking survivin show disrupted microtubule formation and became polyploid (22). HeLa cells transfected with CENP E siRNA revealed defects in chromosome congression to the spindle equator and production of multipolar arrays (23). The mitotic phenotypes observed after Orc6 siRNA treatment were distinct from those obtained after Orc2 siRNA treatment (9). The latter showed a substantial decrease in bromodeoxyuridine (BrdU) staining (20 to 25% positive for BrdU

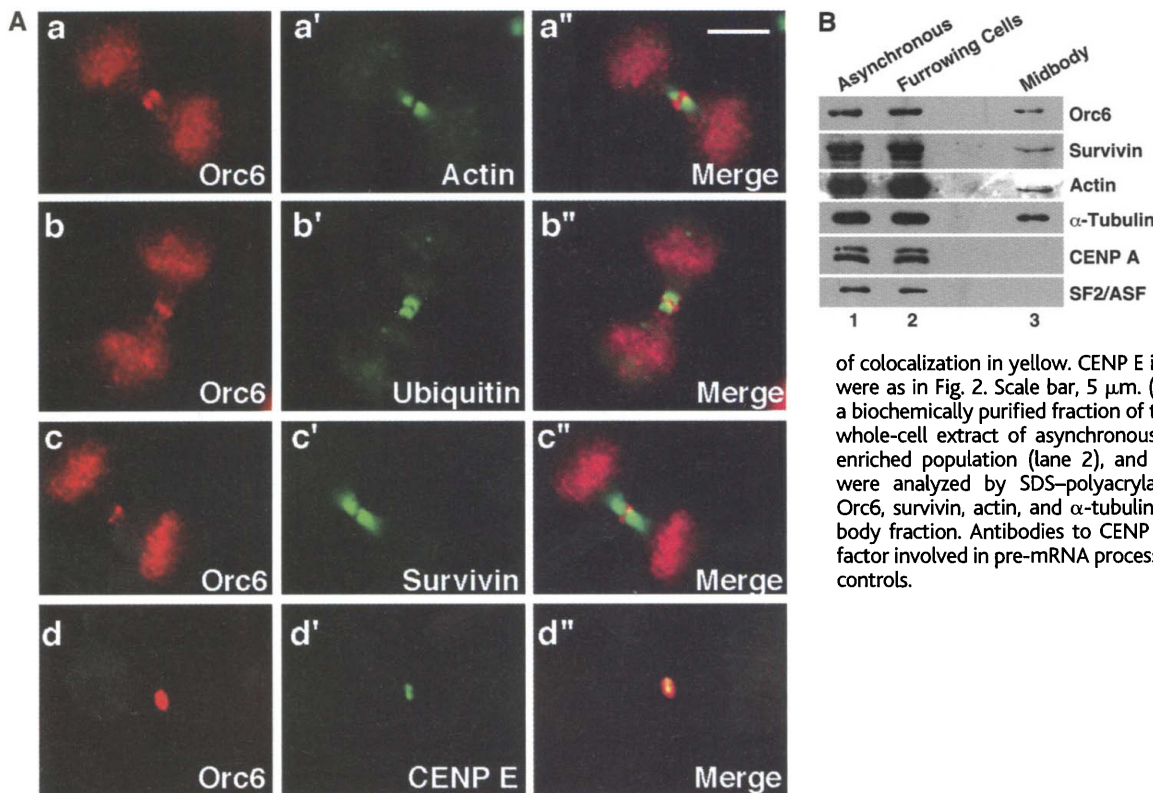


**Fig. 3.** Orc6 concentrates to the midbody region at the Flemming body during human cell cytokinesis. (A) Double-label indirect immunofluorescence staining of HeLa cells for actin (a'), ubiquitin (b'), survivin (c'), or CENP E (d') with Orc6 [in red, (a to d)] in the midbody region during telophase. Corresponding merged images (a'' to d'') show areas

of colocalization in yellow. CENP E immunostaining conditions were as in Fig. 2. Scale bar, 5  $\mu$ m. (B) Immunoblot analysis of a biochemically purified fraction of the midbody. Proteins from whole-cell extract of asynchronous cells (lane 1), telophase-enriched population (lane 2), and midbody sample (lane 3) were analyzed by SDS-polyacrylamide gel electrophoresis. Orc6, survivin, actin, and  $\alpha$ -tubulin were present in the midbody fraction. Antibodies to CENP A and SF2/ASF (a splicing factor involved in pre-mRNA processing) were used as negative controls.

## REPORTS

by 60 hours) and an M-phase arrest, resembling the phenotypes of *Orc2* mutants of treated *Drosophila* (24), but did not show polyploidy and multinucleation (with 4 to 5% multinucleation similar to that seen in control

Gl3 cells). On the other hand, with respect to mitosis and cytokinesis, *Orc6* had similar phenotypes to those of chromosomal passenger and cell cycle checkpoint proteins, further establishing that *Orc6* might play an

important role as an integral component of the cell cycle checkpoint machinery that regulates cytokinesis.

The elimination of *Orc6* also resulted in significantly decreased BrdU incorporation,

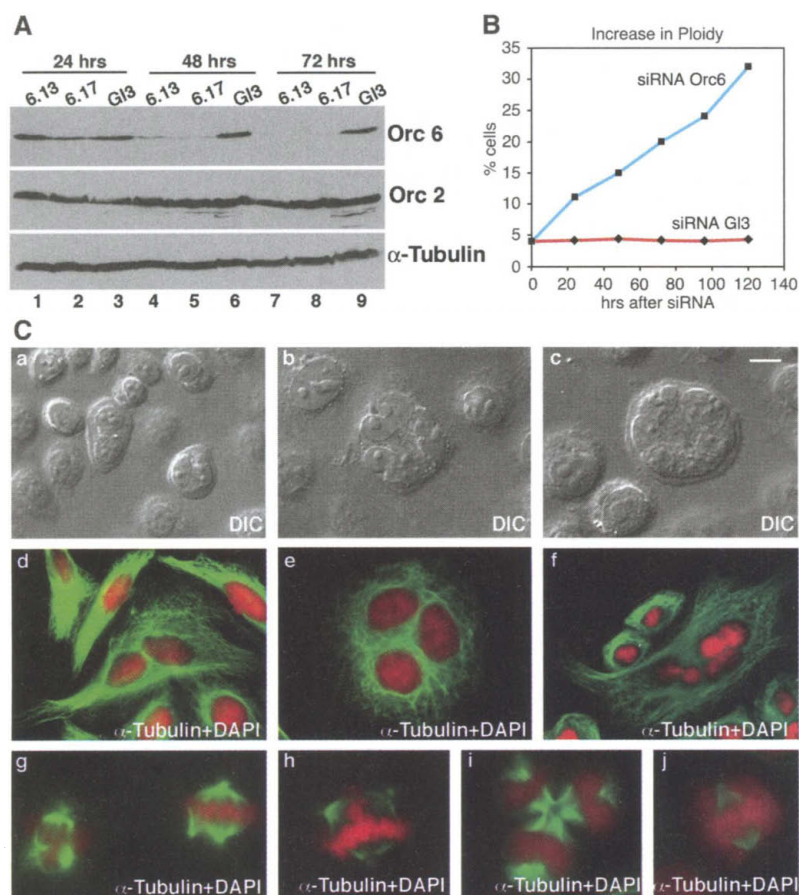


**Fig. 4.** Increased multinucleation upon silencing of *Orc6* expression in HeLa cells by siRNA treatment. **(A)** Immunoblot of whole-cell extract from cells transfected with *Orc6* siRNA duplexes (6.13 and 6.17) or control luciferase (Gl3) and harvested at 24 hours (lanes 1 to 3), 48 hours (lanes 4 to 6), and 72 hours (lanes 7 to 9). Cells were transfected at 0, 24, and 48 hours at about 20% starting confluency. Efficacy of RNAi was assessed by immunoblotting with *Orc6*. *Orc2* and  $\alpha$ -tubulin levels were used as loading controls. **(B)** Time course of percentage of polyploid (multinucleate) cells using oligo 6.17. **(C)** Nomarski micrograph of binucleate (a) and multinucleate cells (b and c).  $\alpha$ -Tubulin (green) and DAPI (red) staining of binucleate cells at 24 hours after *Orc6* siRNA treatment (d), trinucleate cells at 48 hours (e), and multinucleate cells at 120 hours (f) showed these nuclei to be DAPI-positive, although variably in (f). Cells transfected with *Orc6* siRNA showed multipolar spindles (g and h), aberrant mitosis (i), and apparent failure to align chromosomes by 150 hours after *Orc6* siRNA treatment (j) by  $\alpha$ -tubulin staining. Scale bar, 5  $\mu$ m.

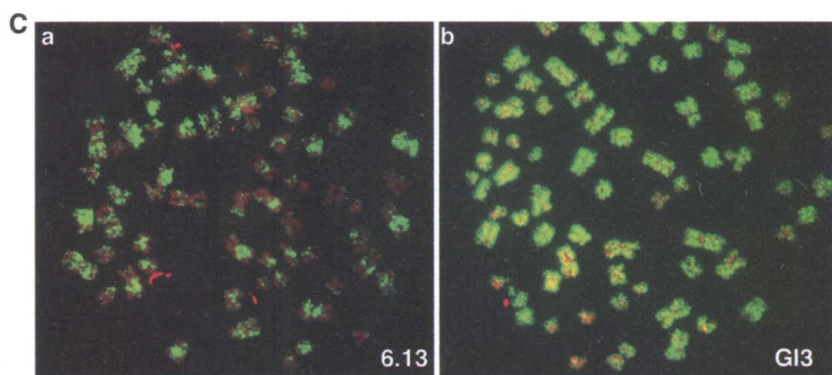
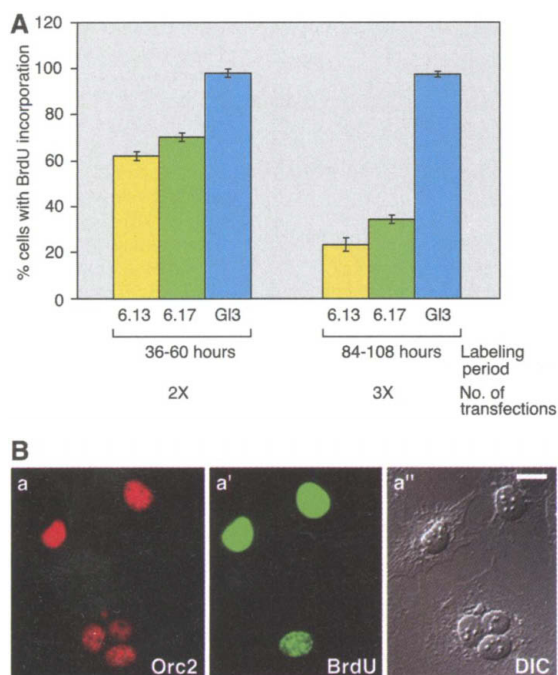


**Fig. 5.** Human *Orc6* silencing causes loss of DNA replication. **(A)** Histogram showing the percentage of cells incorporating BrdU after transfection with *Orc6* (6.13 and 6.17) or luciferase (Gl3) siRNA duplexes. BrdU incorporation was allowed for 24 hours to ensure that all cells had the chance to pass through at least one S phase. **(B)** Multinucleate cells with variable levels and pattern of BrdU incorporation (a'), *Orc2* indirect immunofluorescence for nuclei detection (a), and Nomarski (a''). Scale bar, 5  $\mu$ m. **(C)** Staining of metaphase chromosomes with antibodies to BrdU after a 24-hour BrdU label before colcemid treatment. A punctate pattern of replication in *Orc6* siRNA cells (a) and complete replication pattern in Gl3 control cells (b).

suggesting down-regulation of DNA replication and providing evidence for a role of human Orc6 in DNA replication. BrdU incorporation studies revealed 60 to 70% cells positive for BrdU after 60 hours of transfection, and decreased to 20 to 30% cells after 108 hours (Fig. 5A). In the majority of multinucleate cells, one or two nuclei showed much lower than normal BrdU staining and the remaining nuclei had no BrdU incorporation over a 24-hour period (Fig. 5B). Some cells transfected with Orc6 siRNA duplexes showed an overall intensity of BrdU staining considerably lower than that observed in control cells (see figs. S5 and S6), suggesting infrequent replication origin-firing. Because the origins of DNA replication are redundant, it is likely that most of the Orc6 had to be depleted to reveal a complete defect in DNA replication. BrdU incorporation followed by colcemid-induced metaphase spreads following 108 hours of Orc6 siRNA showed incomplete and lower levels of BrdU incorporation during a 24-hour label (Fig. 5C) (fig. S7). However, the control cells (GI3) showed complete staining of duplicated chromosomes. The punctate incorporation of BrdU suggests that fewer origins fire, resulting in a slower S phase. Similarly, *Drosophila* larvae homozygous for Orc2 and Orc5 mutants progressed slowly through S phase and showed vastly reduced BrdU incorporation; these defects may have been caused by fewer active origins (24).

In human cells, Orc6 functions in multiple aspects of the cell division cycle, including DNA replication, chromosome segregation, and cytokinesis. It may be that Orc6 participates independently in the mechanics of DNA replication, centromere function, and cytokinesis. Alternatively, a significant defect in DNA replication caused by silencing of Orc6 might trigger aberrant mitosis (or other downstream effects) by interfering with centrosome duplication (25). Although this scenario could explain the spindle defects and polyploidy, it would not explain the cytokinesis defects in cells lacking Orc6. A reduction in DNA replication after Orc2 siRNA treatment did not yield similar phenotypes. Also, the Orc6 siRNA phenotypes are consistent with Orc6 distribution to the kinetochores and midbody. A third possibility is consistent with the Orc6 localization pattern during the cell cycle: Orc6 could be essential for inducing or signaling to multiple cell cycle checkpoints that coordinate the many processes of the cell division cycle (26). In this model, chromosome duplication, segregation, and cytokinesis would be coordinated by a common participant. A protein such as Orc6 could cycle from origins of DNA replication to centromeres and the cytokinesis apparatus to ensure the correct order and coordination of events.

References and Notes

1. S. Waga, B. Stillman, *Annu. Rev. Biochem.* **67**, 721 (1998).  
 2. S. P. Bell, *Genes Dev.* **16**, 659 (2002).

3. ———, B. Stillman, *Nature* **357**, 128 (1992).  
 4. T. J. Kelly, G. W. Brown, *Annu. Rev. Biochem.* **69**, 829 (2000).  
 5. I. Chesnokov, M. Gossen, D. Remus, M. Botchan, *Genes Dev* **13**, 1289 (1999).  
 6. I. Chesnokov, D. Remus, M. Botchan, *Proc. Natl. Acad. Sci. U.S.A.* **98**, 11997 (2001).  
 7. J. Mendez *et al.*, *Mol. Cell* **9**, 481 (2002).  
 8. A. A. Van Hooser, M. A. Mancini, C. D. Allis, K. F. Sullivan, B. R. Brinkley, *FASEB J.* **13** (suppl. 2), S216 (1999).  
 9. S. G. Prasanth, B. Stillman, unpublished data.  
 10. D. A. Skoufias, P. R. Andreassen, F. B. Lacroix, L. Wilson, R. L. Margolis, *Proc. Natl. Acad. Sci. U.S.A.* **98**, 4492 (2001).  
 11. M. Glotzer, *Annu. Rev. Cell Dev. Biol.* **17**, 351 (2001).  
 12. S. G. Zeitlin, K. F. Sullivan, *Curr. Biol.* **11**, R514 (2001).  
 13. P. Fortugno *et al.*, *J. Cell Sci.* **115**, 575 (2002).  
 14. J. M. Mullins, J. R. McIntosh, *J. Cell Biol.* **94**, 654 (1982).  
 15. W. C. Earnshaw, R. L. Bernat, *Chromosoma* **100**, 139 (1991).  
 16. D. G. Lee, S. P. Bell, *Mol. Cell. Biol.* **17**, 7159 (1997).  
 17. M. Weinreich, C. Liang, H. H. Chen, B. Stillman, *Proc. Natl. Acad. Sci. U.S.A.* **98**, 11211 (2001).  
 18. P. J. Gillespie, A. Li, J. J. Blow, *BioMed Central Biochem.* **2**, 15 (2001).  
 19. S. M. Elbashir *et al.*, *Nature* **411**, 494 (2001).  
 20. Orc6 siRNA oligos 6.13 (5'-AAUGGUAGCCACAUCGGUGU-3') and 6.17 (5'-AAGATTGGACAGCAGGUCGAC-3') were obtained from Dharmacon Research Inc.  
 21. R. R. Adams, H. Maiato, W. C. Earnshaw, M. Carmena, *J. Cell Biol.* **153**, 865 (2001).  
 22. A. G. Uren *et al.*, *Curr. Biol.* **10**, 1319 (2000).  
 23. J. Harborth, S. M. Elbashir, K. Bechert, T. Tuschl, K. Weber, *J. Cell Sci.* **114**, 4557 (2001).  
 24. M. F. Pflumm, M. R. Botchan, *Development* **128**, 1697 (2001).  
 25. O. C. Sibon, A. Kelkar, W. Lemstra, W. E. Theurkauf, *Nature Cell Biol.* **2**, 90 (2000).  
 26. H. Murakami, P. Nurse, *Biochem. J.* **349**, 1 (2000).  
 27. S. A. Jablonski, G. K. Chan, C. A. Cooke, W. C. Earnshaw, T. J. Yen, *Chromosoma* **107**, 386 (1998).  
 28. We thank all members of the Stillman laboratory for stimulating discussions; H. Zou-Yang and S. Dike for anti-ORC antibodies; T. J. Yen, B. R. Brinkley, K. H. A. Choo, and F. McKeon for kinetochore antibodies; A. Krainer for SF2/ASF antibody; D. L. Spector and D. Helfman for suggestions; J. Mendez, A. Stenlund, and G. Hannon for reading the manuscript; and J. Duffy for artwork and photography. Supported by National Cancer Institute grant CA13106.

Supporting Online Material

www.sciencemag.org/cgi/content/full/297/5583/1026/DC1  
 Figs. S1 to S7

11 April 2002; accepted 22 May 2002

# Impaired B and T Cell Antigen Receptor Signaling in p110δ PI 3-Kinase Mutant Mice

Klaus Okkenhaug,<sup>1</sup> Antonio Bilancio,<sup>1\*</sup> Géraldine Farjot,<sup>1\*</sup> Helen Priddle,<sup>2\*†</sup> Sara Sancho,<sup>3</sup> Emma Peskett,<sup>1</sup> Wayne Pearce,<sup>1</sup> Stephen E. Meek,<sup>2</sup> Ashreena Salpekar,<sup>1</sup> Michael D. Waterfield,<sup>1,4</sup> Andrew J. H. Smith,<sup>2</sup> Bart Vanhaesebroeck<sup>1,4‡</sup>

Class IA phosphoinositide 3-kinases (PI3Ks) are a family of p85/p110 heterodimeric lipid kinases that generate second messenger signals downstream of tyrosine kinases, thereby controlling cell metabolism, growth, proliferation, differentiation, motility, and survival. Mammals express three class IA catalytic subunits: p110α, p110β, and p110δ. It is unclear to what extent these p110 isoforms have overlapping or distinct biological roles. Mice expressing a catalytically inactive form of p110δ (p110δ<sup>D910A</sup>) were generated by gene targeting. Antigen receptor signaling in B and T cells was impaired and immune responses in vivo were attenuated in p110δ mutant mice. They also developed inflammatory bowel disease. These results reveal a selective role for p110δ in immunity.

There is increasing evidence for an important role for class IA PI3Ks in regulation of the immune system (1–4). Mice lacking the

p85α regulatory subunit show impaired B cell development and activation but normal T cell activation, whereas T cell-restricted deletion of the gene for the phosphoinositide 3-phosphatase PTEN, a negative regulator of PI3K signaling, results in a lethal lymphoproliferative disease (5–7). To date, the specific role for each of the three class IA PI3K catalytic subunits in lymphocyte signaling has not been determined. p110δ is expressed predominantly in leukocytes (8, 9), which indicates that it may play a unique role in immune signaling.

The study of class IA PI3Ks is complicated by the heterodimeric nature of these proteins,

<sup>1</sup>Ludwig Institute for Cancer Research, 91 Riding House Street, London W1W 7BS, UK. <sup>2</sup>Gene Targeting Laboratory, Center for Genome Research, University of Edinburgh, West Mains Road, Edinburgh, EH9 3JQ, UK. <sup>3</sup>Primorfo, Rue du Musée 12, CH-1705 Fribourg, Switzerland. <sup>4</sup>Department of Biochemistry and Molecular Biology, University College London, Gower Street, London WC1E 6BT, UK.

\*These authors contributed equally to this report.  
 †Present address: Roslin Institute, Roslin, Midlothian, EH25 9PS, UK.  
 ‡To whom correspondence should be addressed. E-mail: bartvanh@ludwig.ucl.ac.uk